

I. Background and context of the research

Thin films of polycrystalline diamond are finding ever increasing technological uses as for example, wear resistant coatings and infra-red windows and have an expanding range of electronic and electrochemical applications.^{1,2} Such films are grown by chemical vapour deposition (CVD) and most diamond CVD involves activation of a dilute hydrocarbon / H₂ mixture (e.g. 1% CH₄ in H₂) at a pressure of a few tens of Torr, and subsequent growth on the chosen substrate material maintained at an elevated temperature (typically ~800°C).³ Essential to such growth processes is the formation of H atoms in the reacting mixture. In a hot filament (HF) reactor, H atoms are created by thermal dissociation at the filament surface, whereas in microwave or DC-arc activated plasma devices H atoms are formed by a combination of thermal dissociation of H₂ and dissociation via collisions with high-energy electrons, ions and metastables in the plasma. These H atoms are accredited with several key growth roles. Crucially, they can react with the hydrocarbon precursors to produce carbon (C₁) based radicals (e.g. C atoms or CH₃) that adsorb onto, and react with, the substrate and subsequently the growing film. C₁ radicals also react with each other to form C₂ species and higher hydrocarbons and radicals. The chemistry of the gaseous environment ultimately determines the nature of the deposited film – only under a narrow range of processing conditions are diamond films successfully deposited in competition with graphitic and diamond-like carbon (DLC) materials. This chemistry is highly complicated, and there is considerable uncertainty about the mechanisms of film growth at the gas-surface interface.

In the program of research supported by GR/M67506, the activated regions of an HF reactor and a 10 kW DC arc jet reactor, both used for CVD of thin, polycrystalline diamond films, have been probed by cavity ring-down spectroscopy (CRDS). The two types of reactor offer very contrasting levels of gas phase activation and species concentrations, and potentially very different diamond growth mechanisms. Laser-based CRDS enables quantitative measurements of **absolute concentrations** of radicals and molecules, mapping of their spatial distributions, and determinations of local gas temperatures. CRDS is an absorption-based spectroscopic method and hence is very general in its applicability. Thus, we have been able to study a variety of radicals and molecules present in the two reactors and have learned a great deal about the gas phase chemistry that leads to thin film deposition. The HF reactor served as a test instrument for development of experimental methods, but also yielded many novel results that have been used to refine computer models of the chemistry of the CVD process. The DC arc jet reactor produces a highly activated, luminous gaseous plume consisting of atoms, radicals, molecules and charged particles, and our experiments generated considerable data that have stimulated construction of new computer models to aid understanding of this extreme environment.

We have successfully demonstrated the use of two variants of the CRDS technique to make quantitative measurements of the activated gas mixtures. The first of these variants, continuous wave (cw) CRDS, exploits tuneable near infra-red (IR) diode lasers, and was the method emphasised in the original grant application. For reasons largely motivated by technical problems with the commercial diode lasers (outlined in section III) we also initiated a programme of CRDS measurements using UV and visible light from a pulsed dye laser system. Numerous, highly complementary results have been forthcoming from these two strands of the project, and have prompted considerable activity by colleagues from Moscow State University, Drs Y.A. Mankelevich (YAM) and N.V. Suetin (NVS), who are developing computer models of the activation, flow dynamics and chemistry of these CVD environments. The quantitative CRDS measurements of absolute concentrations and temperatures provide critical tests of computer models and thus substantial refinement of these models has been possible. The mutual benefits for the Bristol and Moscow groups will be illustrated in sections II and IV of this report.

II. Key advances and support methodology

Both a hot filament reactor and a DC arc jet reactor used for thin diamond film CVD were modified to accommodate adjustable mounts for the mirrors required for CRDS experiments. The mirror mounts were separated from the main reactor chambers by flexible edge-welded bellows, and the tilts of the flanges were finely controlled by the use of micrometers to enable optimum alignment of the ring-down cavity (RDC) formed by two mirrors. The RDCs were aligned to intersect the activated region of the HF reactor or the middle of the arc jet plume. The same RDC set-up was used for both cw and pulsed laser experiments, but the optical systems differed, as shown schematically in figure 1. This section is sub-divided into descriptions of the progress made with the two separate CRDS techniques.

The HF reactor employs a 250 µm diameter Ta wire filament powered by a DC supply and mounted on a linear transfer mechanism allowing vertical translation by ≤25 mm. The HF temperature (T_{fil} , typically 2150°C) is monitored by a two-colour optical pyrometer. Feed gases (1%CH₄ / H₂) are delivered via mass flow controllers that maintain an overall flow rate of 100 sccm and a chamber pressure of 20 Torr, giving film growth rates of ~ 1 µm h⁻¹.

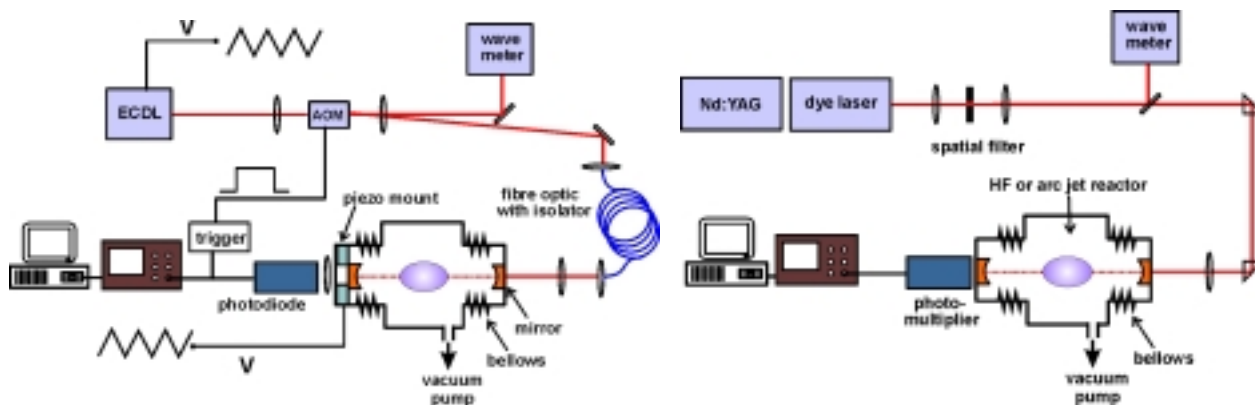


Figure 1: Schematic diagrams of the optical set-ups for the cw CRDS (left) and pulsed laser CRDS (right) experiments

The DC-arc plasma jet reactor consists of a water cooled stainless steel chamber with several quartz viewing ports and two extended arms on which the micrometer adjustable mirror mounts are attached. The 28-mm diameter molybdenum substrate for film growth is mounted on a long, water-cooled steel tube and its position in the chamber can be translated (by up to ± 20 mm) in three dimensions. The torch head assembly is mounted on a large copper flange and faces the substrate. The twin torch consists of an N-torch through which the primary flow of Ar is mixed with a secondary spiral stream of Ar / H₂. Perpendicular to the N-torch is the smaller P-torch through which a further stream of Ar is added to the jet. Total gas throughputs are typically 10 slm of Ar in the primary flow through the N-torch, with a further 0.75 slm through the P-torch and a 1.4 slm Ar / 1.8 slm H₂ mix in the secondary N-torch flow. The total pressure in the reactor is maintained at 50 Torr. The plasma is initiated by a DC-arc across the torch nozzles, with typical powers supplied being 5 – 6 kW, though the arc-jet is designed to operate at up to 10 kW. Methane (60 sccm, i.e. 3.3% of the total flow of H₂ for optimal diamond growth) is introduced to the H₂/Ar plasma through a circular injection ring located 100 mm downstream of the nozzle, thereby preventing amorphous carbon deposition on the nozzles.

II.1 cw diode laser CRDS

For both CVD reactors, laser wavelengths in the region of $1.51 \mu\text{m}$ (6610 cm^{-1}) from an external cavity diode laser (ECDL) were used to probe individual rotational lines of the $\nu_1 + \nu_3$ vibrational combination band of acetylene. Approximately 50% of the laser probe beam was deflected off axis by an 80 MHz acousto-optic modulator (AOM) into a single mode fibre optic that contained an optical isolator. The output end of the fibre was positioned in front of one of the cavity mirrors ($R > 99.97\%$) and the output light ($\sim 250 \mu\text{W}$) collimated using an $f = 5$ mm lens. A second, $f = 50$ cm lens was used to focus the laser toward the centre of the cavity to encourage preferential excitation of the TEM₀₀ cavity mode. In the HF reactor, the cavity axis was parallel to the long axis of the coiled filament, and in the DC arc jet reactor, the centre lines of the cavity and gas plume crossed at 90° . The level of laser light leaking from the cavity was continuously monitored by a fibre optic, position behind the opposing cavity mirror, coupled to a fast response photo-diode detector. A vital feature of using a fibre optic to collect the signal is the strong discrimination against background radiation from the hot reactor because of precise directional alignment of the fibre to the probe beam. Either the laser frequency or the cavity length was modulated at 100 Hz, and when the laser and cavity modes passed through resonance and sufficient light built up in the cavity, the AOM was triggered to extinguish the deflected beam and the light within the cavity decayed exponentially with ring-down rate coefficient, k , dependent on the mirror reflectivities, the length of the cavity, ℓ , and the presence of any absorbing media. Mirror losses were quantified, and changes in rate coefficient, Δk , observed when tuning across an absorption line were converted into absorbance, thereby enabling measurement of absolute concentrations of absorbers. Scanning the laser wavelength and measuring Δk at each frequency generated a spectrum. Data were acquired by a digital oscilloscope and coupled into a LabView program on a pc where individual ring down events were fitted to an exponential function and the resultant k values averaged. Wavelength calibration was achieved using a wavemeter. The modulation and the scanning of the laser frequency were controlled by an analogue voltage interfaced via a data acquisition card.

Spectra of individual rotational lines of the $\nu_1 + \nu_3$ band of C₂H₂ were recorded and fitted to Gaussian functions to derive intensities and linewidths. The full absorption band was simulated using the PGOPHER⁴ software and absolute line strengths at required temperatures were derived from the simulations by scaling from 296 K literature values.

II.1.A Gas Temperatures

The full width at half maximum (FWHM, $\Delta\nu$) of each absorption line scan was obtained from the line shape and, from the Doppler broadening, an effective gas temperature (T_{gas}) that is the average along the line of sight of the laser beam can be derived. A sample line profile of the R(22) line centred at 6603.41 cm^{-1} is shown in figure 2, together with a fit. The deduced FWHM is $\Delta\nu = 0.022 \pm 0.003 \text{ cm}^{-1}$ ($650 \pm 90 \text{ MHz}$). Instrumental contributions to the line width are

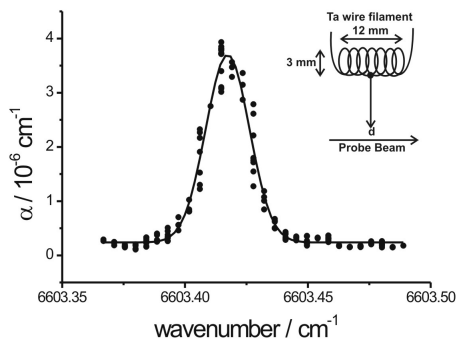


Figure 2: An example of a cw CRD spectrum of C_2H_2 in the HF reactor.

II.1.B Absolute concentrations

Number densities averaged along the path of the probe beam can be calculated from CRD spectra because $\Delta k_{\bar{\nu}}$ at any laser wavenumber ($\bar{\nu}$) is related to the absorption coefficient, $\alpha_{\bar{\nu}}$, at that wavenumber by:

$$\alpha_{\bar{\nu}} = \frac{\Delta k_{\bar{\nu}} \ell}{c l} \quad (1)$$

where ℓ is the mirror separation and l is the effective absorption length of the column containing C_2H_2 . Absorption coefficients, integrated across spectral lines, were converted to absolute concentrations of C_2H_2 using careful determination of the T -dependent absorption cross sections for single rotational lines, $\sigma_{int}(T)$:⁶

$$[C_2H_2] = \frac{\int \alpha_{\bar{\nu}} d\bar{\nu}}{\sigma_{int}(550 \text{ K})} \quad (2)$$

Under standard growth conditions in the HF reactor (1% CH_4 in H_2 , $p = 20$ Torr, $T_{fil} = 2150^\circ C$) the average acetylene number density is $(2.9 \pm 0.6) \times 10^{13}$ molecules / cm^3 . This equates to $\sim 1.7\%$ of the total carbon fed in as CH_4 and compares well with preliminary 2-D model calculations (by YAM and NSV) predicting $\sim 6.5 \times 10^{12}$ molecules / cm^3 . The deduced average number density of C_2H_2 in the arc jet (0.5% CH_4 in H_2 and excess Ar, 50 Torr, 5.8 kW discharge power) is $(1.2 \pm 0.2) \times 10^{14}$ molecules / cm^3 , corresponding to some 40% of the total carbon feed. The large difference in the respective methane \rightarrow acetylene conversion efficiencies in the two systems reflects the very different volumes of, and gas temperatures in, the activated regions of the different reactors. In the HF reactor, the thermally activated chemistry is confined primarily to a small cylindrical region about the filament with length determined by the filament coil (~ 12 mm) and extending ~ 15 mm radially.⁵ Thus, a large fraction of the flow of feed gases, introduced above the filament region, passes through the reactor to the exhaust line without sampling this volume. Conversely, in the DC arc jet, the plume volume is defined by the diameter (≥ 12 mm) and length (typically 150 mm) of the plume, the flows of H and H_2 are largely confined to the plume by the nozzle expansion, and CH_4 addition is by expansion from a ring surrounding the plume axis to encourage CH_4 entrainment. The abundance of H atoms in the high temperature plume encourages rapid removal of successive hydrogen atoms from CH_4 to form a high density of C atoms that react with CH to make C_2 and ultimately leads to production of C_2H_2 and higher C_xH_y ($x \geq 3$) species.

Spatial variations of the C_2H_2 number densities and temperatures were probed in both reactors, but they were found to be *independent* of distance from the HF or arc jet substrate. These observations should be contrasted with measurements of the spatial variations of densities and temperatures of radical species (CH_3 , NH , C_2 and CH) that we made by pulsed laser CRDS in the same reactors (see section II.2) and further encourage the conclusion that acetylene is present throughout the entire volume of both chambers whereas the radicals are localized in the activated regions.

II.1.C. The effects of reactor operating parameters

Two operating parameters of the reactors that can be varied to learn more about the activation and chemistry of the gas phase component of the CVD process are the percentage of methane in the feedstock gas and the input power.

Feed gas methane fraction: In the HF reactor, absorption profiles of the R(22) line of the $\nu_1 + \nu_3$ C_2H_2 band were scanned for various CH_4/H_2 input ratios. Integration of line intensities and conversion to C_2H_2 number densities gave the data plotted in fig. 3(a). Similar measurements using the R(26) C_2H_2 line were repeated in the arc jet reactor for CH_4/H_2 ratios of 0.4–0.8%, yielding the data plotted in fig. 3(b). In both cases there is a monotonic rise in the concentration of C_2H_2 as the fraction of added CH_4 increases. The C_2H_2 acts as a carbon reservoir with low reactivity

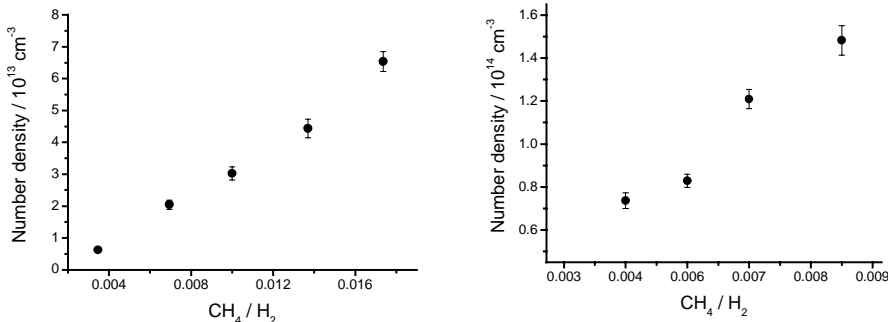


Figure 3: Variations of [C₂H₂] with added CH₄ (a) HF, and (b) DC arc jet reactor.

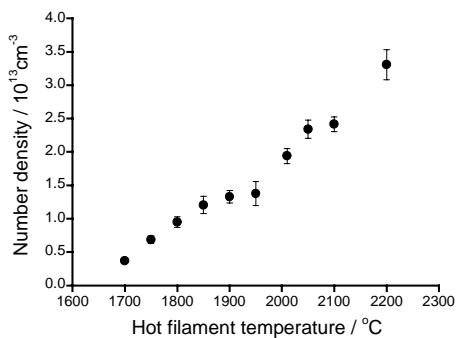


Figure 4: Variation of [C₂H₂] with T_{fil} .

conditions of 1% CH₄ in H₂ at 20 Torr. Analysis of the Doppler widths of spectral lines, however, shows no variation about a mean C₂H₂ temperature of ~550 K, despite variation of T_{fil} from 1700–2200°C. The quality of data obtained from power dependent studies in the DC arc jet was lower, because of instabilities in its operation over the timescale of the measurements, but the variation of C₂H₂ concentrations with input power ranging from 4.6 – 8.0 kW for a 0.5% CH₄/H₂ ratio illustrates a weak trend to greater C₂H₂ production at higher arc jet powers. As was observed for the HF reactor, however, the Doppler widths of the acetylene absorption lines show no discernable variation with input power, and exhibit a mean T_{gas} of ~ 550 K.

Increased T_{fil} or arc jet power promotes H-atom formation that drives the chemistry towards C₂H₂ production. The insensitivity of the measured C₂H₂ temperatures to T_{fil} or input power supports the assertion that the C₂H₂ is widely distributed in the reactor and that we measure an average temperature sampled through the changing activated region and the larger, but invariant and cooler, surrounding stagnation volumes. The C₂H₂ is created in the central, activated region and hence takes time to diffuse outward. It is also continuously removed by pumping of the reactor to maintain the 100 sccm / 20 Torr flow rate and pressure in the HF reactor or ~14 slm / 50 Torr in the arc jet reactor. The timescales of these production, diffusion and loss processes have been measured in both reactors by monitoring C₂H₂ absorbance as a function of time after switch-on and switch-off of the HF current or the CH₄ flow (arc jet) and were successfully modelled in terms of diffusion and pump-out processes.⁶ It is clear that the steady state C₂H₂ concentration must be included in models as an additional source of C-containing compounds to the activated region.

II.2 Pulsed laser CRDS

Experiments employed an existing Nd:YAG pumped dye laser system to record spectra, concentrations and spatial distributions of CH₃ (at 214 nm), NH (at 336 nm), C₂ (at 515 nm) and CH (at 427 nm). Absorptions attributed to C₃ radicals were also observed in the 427-nm region. Measurements of CH₃ and NH were restricted to the HF reactor, CH was studied in both CVD reactors, and C₂ was probed in the arc jet plume. Results are summarised below to illustrate the scope of the experiments. The emphasis is placed on measurements in the DC arc jet because this is a true technological plasma, and the outcomes of measurements in the HF reactor are mentioned only very briefly.

Pulsed UV CRDS was used to measure CH₃ formed in the HF reactor from 1% CH₄/H₂ and 1% C₂H₂/H₂ gas mixtures, and the results were modelled quantitatively by YAM and NVS. Concentrations of CH₃ were shown to decline from 1.1×10^{14} to 1×10^{13} molecules cm⁻³ over the range of distances from the filament $d = 0 - 10$ mm. NH was also studied in a 1%CH₄/H₂ gas mixture incorporating 5% NH₃ as part of an investigation of the chemistry leading to possible N-incorporation in diamond films. A careful comparison of model predictions and experimental data, allowing for variations in T_{gas} and radical density along the viewing column of the laser beam, showed extraordinary agreement (to within 20%) for NH number densities and their dependence on distance from the filament.⁷

Spectra of C₂ in the arc jet were recorded via the $d^3\Pi_g - a^3\Pi_u$ Swan bands and CH spectra were obtained for a few rotational lines of the $A^2\Delta - X^2\Pi$ transition. Spectra were analysed to obtain temperatures, radical concentrations, and their variation with position in the plume and with the process parameters of the DC arc jet, as illustrated below.

II.2.A Gas temperatures

Intensities of isolated rotational lines in the C₂ and CH absorption spectra were integrated by fitting to Gaussian functions. The measured C₂ line intensities, together with computed line strengths, were used in Boltzmann plots to derive rotational temperatures. These are averaged along the line of sight of the absorption measurements and

and all the carbon chemistry leading to C₂H₂ formation will be promoted by increased methane inputs.

Input power: The input power to the HF reactor is controlled by current and voltage settings for the electrical supply to the filament, and determines the filament temperature (T_{fil}), which is measured by a pyrometer. Figure 4 shows the pronounced dependence of the C₂H₂ number density (from integrated R(22) rotational line intensities) on T_{fil} for otherwise standard operating

therefore should contain contributions from both the hotter central core of the arc jet and the cooler outer regions, but yield an average temperature of 3300 ± 200 K. This temperature is consistent with the experimentally measured Doppler broadened C_2 linewidths of 0.16 ± 0.01 cm^{-1} from which a temperature of 3200 ± 300 K is calculated. Analysis of Doppler widths demonstrates a uniform gas temperature for distances $z > 5$ mm from the substrate, but local heating of the gas for $z < 5$ mm and temperatures estimated to rise as high as 4800 ± 400 K at $z = 1$ mm.

II.2.B $C_2(a)$ and $CH(X)$ concentrations

The changes in the ring-down time measured as the laser frequency is scanned across a line profile can be used to determine absorption coefficients at each frequency using equation (1), with l the effective absorption length (across the plume) of the column containing $C_2(a)$ or $CH(X)$ radicals and Δk the difference between the ring down rate coefficients on and off the spectral absorption line. Optical emission spectroscopy (OES) guided the choice of $l = 1$ cm. From simulations of the $C_2(d-a)$ spectrum we can calculate the fraction, p , of the total ($v'=0-v''=0$) band oscillator strength that is associated with each monitored rotational line at this temperature. The known Einstein A-coefficient for the (0-0) band, A_{00} , is then related to the integrated absorption coefficient of the line of interest by

$$\int_{\text{line}} \alpha_{\bar{\nu}} d\bar{\nu} = \frac{\lambda^2}{8\pi c} \frac{g_d}{g_a} [C_2(a, v=0)] A_{00} p \quad (3)$$

where g_d and g_a are the electronic degeneracies of the d- and a-states. $[C_2(a, v=0)]$, the concentration of $C_2(a)$ radicals in their lowest vibrational level, can thus be deduced and multiplication by the (T -dependent) vibrational partition function calculated at 3300 K yields the total $C_2(a)$ concentration, $[C_2(a)]$. Analysis of lines in the spectrum returns $[C_2(a)] = 1.5 \pm 0.2 \times 10^{13}$ cm^{-3} , for an input power of 6.5 kW and a CH_4/H_2 ratio of 3.3%. These C_2 concentrations are

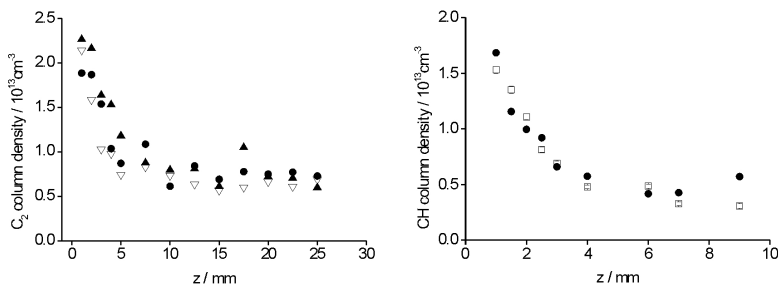


Figure 5: Variations of $[C_2]$ and $[CH]$ with distance from the substrate. The various symbols correspond to data from different spectral lines.

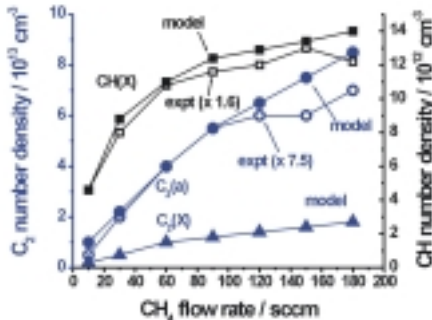


Figure 6: Model and experimental variations of $[C_2]$ and $[CH]$ with added CH_4 . Note the scaling of the experimental data to the model values, and the excellent agreement in trends with CH_4 flow rate.

from model calculations by YAM and NVS, and show initial rises in radical concentrations that plateau beyond 100 sccm CH_4 flows. As the input power in the reactor increased from 5.25 to 8.4 kW, $[C_2]$ increased monotonically, but the $[CH(X)]$ was almost invariant. Higher gas temperatures might be expected to result from increased input power, but Doppler broadened C_2 lines show only a very small increase in width over the range of powers studied.

Existing kinetic models neglect the possible role of C_2 in diamond film growth (though the new mechanisms used in the calculations of YAM and NVS now remedy this deficiency), but *ab initio* calculations show that addition of C_2 to both H-terminated and unterminated diamond (110) surfaces are exothermic and barrierless processes. Boundary layer thickness influences the growth species because of loss of C atoms in the boundary layer and formation of CH_3 radicals. The high velocities of arc jets give thin boundary layers and thus these reactors are predicted to operate in a regime of rapid film growth by C atoms. The presence of C_2 in the arc jet plume at concentrations up to $\sim 10^{13}$ cm^{-3} , and the increase in its concentration in the (thin) boundary layer encourage its consideration as a growth species.

III. Project plan review

The original purpose of the proposed research was to develop diode laser CRDS, making use of compact, near IR, cw solid-state laser sources, as a diagnostic method to learn about chemistry in thermally and plasma activated gas

mixtures. This objective has been achieved, with successful study of C₂H₂ in both the HF and DC arc jet reactors. Early stages of the project were, however, beset by problems with the diode lasers. The company EOSI from which two external cavity diode lasers were purchased, was bought out by Newport and, as a result, technical support for the ECDLs was cut. The first two diode lasers were damaged in shipping, we also suffered premature failures in the laser diodes, and were faced with waiting periods of up to 6 months for replacements. We resolved these problems in two ways: (i) additional diode lasers were purchased from a German company, Sacher Lasertechnik, which proved to be more reliable; (ii) we extended the boundaries of the project to include pulsed laser CRDS studies of radical species in the two reactors. The adaptations to the reactor chambers for cw CRDS experiments were also appropriate for the pulsed laser work, and the Bristol group was equipped with an appropriate Nd:YAG and dye laser system, so the pulsed laser experiments were a natural addition to our work with the diode lasers. The two experiments together provided very complementary data on molecular and radical constituents of the two reactors. Anticipated cw CRDS measurements of CH₃, HCN and CH₄ have not yet been made, nor have studies been performed on a microwave reactor. We have, however, developed a cw CRD set-up to probe CH₄ in a range of environments, and have acquired a new microwave plasma chamber which will be adapted in the near future for CRDS experiments.

IV. Research impact and benefits to society

Primary beneficiaries were identified in the proposal as being scientists requiring new techniques to study hostile environments such as flames and plasmas, and those constructing numerical models of the activation, gas-phase chemistry and flow properties of the reactors. We have demonstrated for the first time the use of cw CRDS as a plasma probe, and the use of pulsed laser CRDS to study a diamond depositing arc jet. In both instances, the experiments generate quantitative measurements of absolute concentrations, as well as temperatures and spatial profiles. The sensitivity of the technique is very well suited to experiments of this type and we expect our success to encourage related studies. Through our participation in the Intersect Faraday Partnership (which promotes development of new sensor technologies) and the proposed Faraday Partnership for development and application of plasma techniques, we expect our work to impact on UK science and industry in the near future. The highly productive collaboration with Russian colleagues YAM and NVS has shown the value of our data to computer modellers and has already resulted in 3 joint publications that break new ground in understanding the CVD chemistry in the HF and DC arc jet reactors. YAM has also been stimulated to construct new models of the cascaded arc jet system used for deposition of DLC films by the Plasma Physics group at Eindhoven University of Technology. The two reactors provide interesting comparisons because the chemistry in the Bristol arc jet has been shown to be dominated by reactions of neutral atoms, radicals and molecules, whereas the Eindhoven reactor chemistry is driven largely by ion reactions. In addition, the PG student, Jonathan Wills, was trained in numerous modern scientific techniques, and is now a PDRA in France, having completed his Ph.D and *viva voce* examination in November 2002.

V. Explanation of expenditure

Expenditure followed very closely the proposed budget and there were no significant changes. Travel funds were used by the PI, co-investigator and PG student to attend *Technological Plasma Initiative* meetings each year, and for the PG student to present his work at the *High Temperature Plasma Diagnostics* conference in Wisconsin in July 02.

VI. Further research or dissemination activities

Dissemination during the grant period includes publication of 2 major papers (in the *Journal of Applied Physics*), 1 in press, and 1 submitted, and invited international conference presentations by AJOE (e.g., *4th Frontiers in Low Temperature Plasma Diagnostics Conference*, Holland (2001)) and MNRA (*17th International Gas Kinetics Symposium*, Germany (2002)). Continued funding for related research has been secured from the EPSRC Physics Programme through grant GR/R71726. New challenges include measurement of C₂(X) radicals, spatially resolved measurements perpendicular to the arc jet plume to construct concentration profiles, study of gas mixtures for CVD of carbon nanotubes and nanocrystalline diamond films, and probing of laser ablated plumes used to deposit DLC films.

1. J.E. Field (Ed.), *The Properties of Natural and Synthetic Diamond*, Academic Press, London, 1992, p. 710.
2. B. Dischler and C. Wild (Eds.), *Low-Pressure Synthetic Diamond*, Springer-Verlag, Berlin, 1998, p. 384.
3. D.G. Goodwin and J.E. Butler, in: M.A. Prelas, O. Popovici and L.K. Bigelow (Eds.), *Handbook of Industrial Diamonds and Diamond Films*, Marcel Dekker, New York 1998, pp. 527 – 580.
4. PGOPHER spectral simulation program written by C.M. Western. A summary of the program and the Hamiltonian used is given in M.E. Green and C.M. Western, *J. Chem. Phys.*, 1996, **104**, 848.
5. J.A. Smith, M.A. Cook, S.R. Langford, S.A. Redman and M.N.R. Ashfold, *Thin Solid Films*, 2000, **368**, 169.
6. J.B. Wills, M.N.R. Ashfold, A.J. Orr-Ewing, Y.A. Mankelevich and N.V. Suetin, submitted to *Diamond and Relat. Mater.*
7. J.A. Smith, J.B. Wills, H.S. Moores, A.J. Orr-Ewing, M.N.R. Ashfold, Yu.A. Mankelevich and N.V. Suetin, *J. Appl. Phys.*, 2002, **92**, 672.
8. J. Luque, W. Juchmann, and J.B. Jeffries, *J. Appl. Phys.* **82**, 2072 (1997).